Supporting Information

Stabilization of CVD-grown WS_2 monolayers at elevated temperature with *h*-BN encapsulation

Xiang Hua[1], Datong Zhang[1], Bumho Kim[2], Dongjea Seo[3,4], Kyungnam Kang[5], Eui-Hyeok Yang[5], Jiayang Hu[1], Xianda Chen[1], Haoran Liang[1], Kenji Watanabe[6,7], Takashi Taniguchi[6,8], James Hone[2], Young Duck Kim[9,10,11] and Irving P. Herman[1,*]

[1] Department of Applied Physics and Applied Mathematics, Columbia University, New York, NY 10027, USA
[2] Department of Mechanical Engineering, Columbia University, New York, NY 10027, USA
[3] Department of Materials Science and Engineering, Yonsei University, Seoul 120-749, Korea
[4] Department of Electrical and Computer Engineering, University of Minnesota, Minneapolis, MN 55455, USA
[5] Department of Mechanical Engineering, Stevens Institute of Technology, Hoboken, NJ, 07030 USA
[6] Advanced Materials Laboratory, National Institute for Materials Science, 1-1 Namiki, Tsukuba, 305-0044, Japan
[7] Research Center for Functional Materials, National Institute for Materials Science, 1-1 Namiki, Tsukuba 305-0044, Japan
[8] International Center for Materials Nanoarchitectonics, National Institute for Materials Science, 1-1 Namiki, Tsukuba 305-0044, Japan
[9] Department of Physics, Kyung Hee University, Seoul 02447, Republic of Korea
[10] Department of Information Display, Kyung Hee University, Seoul 02447, Republic of Korea
[11] KHU-KIST Department of Converging Science and Technology, Kyung Hee University, Seoul 02447, Republic of Korea

* Corresponding author, E-mail: iph1@columbia.edu

Section S1. Experimental set up

The experimental set-up is shown in Figure S1. *in situ* PL measurements at different temperatures were performed in real time using $\lambda = 514.5$ nm from a cw argon ion laser. Plasma lines were removed with a notch filter and a low-pass filter. The laser was focused with a 50× objective lenses (Olympus 50× long working distance objective). The focused laser irradiated the sample placed in a Linkam cell (LINKAM THMS 600) with in-situ control of temperature and environment from room temperature to 873 K. Signals were captured by a cryogenically-cooled silicon CCD detector (Princeton Instruments Spec-10:400B).

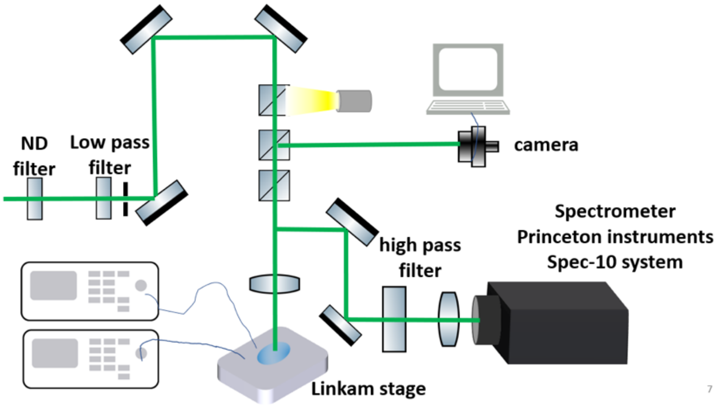

Figure S1. Schematic of the experimental apparatus.

Section S2. Room temperature Raman scattering and photoluminescence in flowing nitrogen and forming gas

To confirm that the WS_2 flakes were not degraded and were well preserved after fabrication, the monolayer of WS_2 flakes were characterized by room temperature Raman scattering and photoluminescence before the start of each run. Figures S2 and S3 respectively show this for flowing nitrogen and forming gas (and Figures 1e and 1f for air).

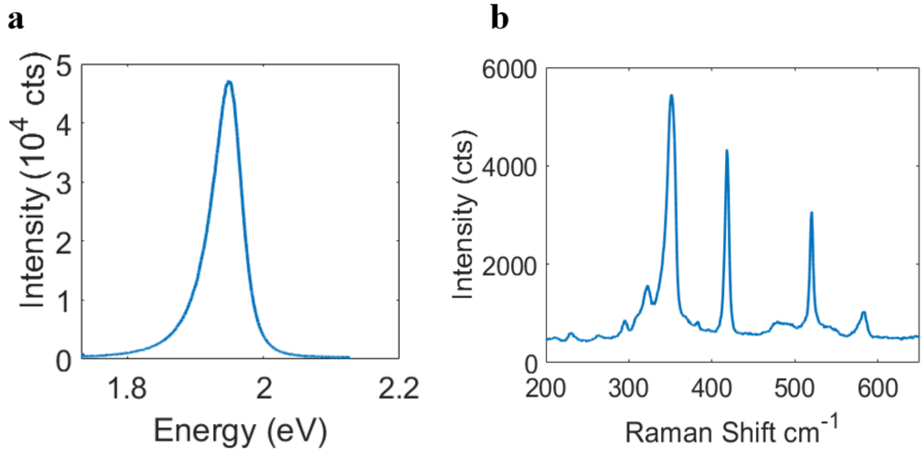

Figure S2. Monolayer WS_2 characterized by (a) PL and (b) Raman scattering at 300 K in flowing N_2

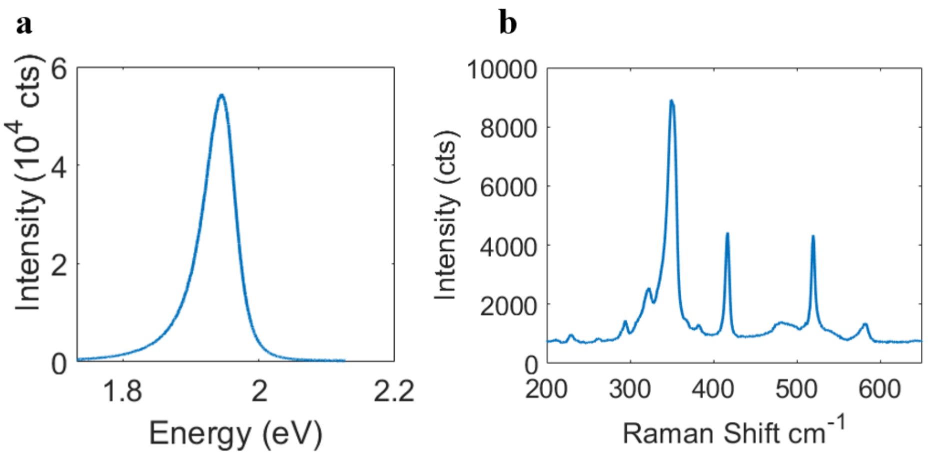

Figure S3. Monolayer WS_2 characterized by (a) PL and (b) Raman scattering at 300 K in forming gas.

Section S3. Raman scattering before and after heating in flowing forming gas

Figure S4 shows the Raman spectra of covered WS_2 at ambient temperature before and after heating to 873 K in forming gas. The three main WS_2 peaks are the 2LA peak at ~352 cm^{-1}, the E_{2g} peak at ~355 cm^{-1}, and the A_{1g} peak at ~417 cm^{-1}. The 520 cm^{-1} peak is from Si. The main *h*-BN peak at ~1380 cm^{-1} is out of range here. There is no evidence for the formation of any products due to the heating process, such as thiols (with main peak at ~850 cm^{-1})[1] or partially reduced SiO_2 (SiO with main peak at 444 cm^{-1} or SiO_{2-x} with a weaker main peak at 520 cm^{-1} than SiO_2)[2,3] – though each may occur but with levels too low to be seen here.

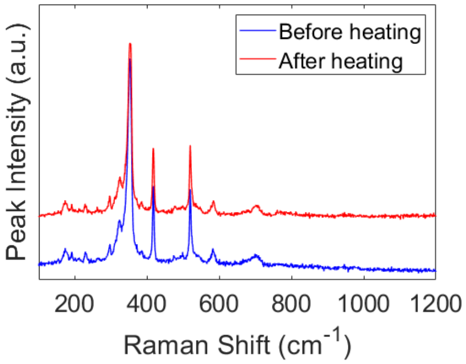

Figure S4. Raman spectra of monolayer WS_2 flakes covered by *h*-BN on the SiO_2/Si substrate at ambient temperature before and after heating to 873 K in flowing forming gas.

Section S4. Optical micrographs before and after heating in flowing nitrogen

Figure S5 shows optical micrographs of covered WS_2 flakes before and after heating in flowing nitrogen. The spots seen in the middle of the flakes after heating in ambient air, in Figure 3b, are not seen here in Figure S5b for flowing nitrogen. (The length of the side of the flake was ~5 μm long in experiments in air and 20-30 μm for those with flowing N_2 and forming gas; this length was not critical as long as the flake was encapsulated by *h*-BN.)

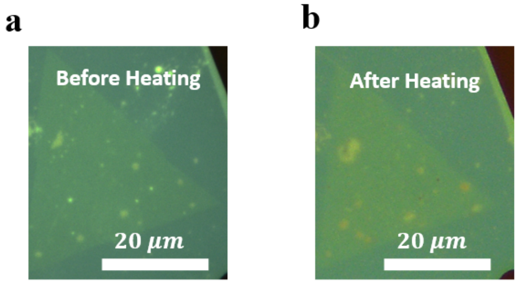

Figure S5. (a) Optical image of WS_2 flakes covered by *h*-BN on SiO_2/Si substrate at ambient temperature (a) before and (b) after heating to 873 K in flowing N_2.

Section S5. The temperature dependence of photoluminescence

The rate equation describing the density of excitons *n* is by: [4,5]

$$\frac{dn}{dt} = G - n(k_r + k_{tr}) \,. \tag{1}$$

G is the optical generation rate, and k_r and k_{tr} are the radiative decay rate and non-radiative rate, respectively. The steady state exciton density is:

$$n = \frac{G}{k_r + k_{tr}} \tag{2}$$

and therefore the photoluminescence intensity can be expressed as:

$$I = \frac{AGk_r}{k_r + k_{tr}} = I_0 \frac{k_r}{k_r + k_{tr}} \, , \tag{3}$$

where A is the collection efficiency. For this two nonradiative recombination channel：

$$I = I_0 \frac{k_r}{k_r + k_{tr1} + +k_{tr2}} = \frac{I_0}{1 + A\, exp\left(-\frac{E_1}{k_B T}\right) + +B\, exp\left(-\frac{E_2}{k_B T}\right)} \, , \tag{4}$$

where

$$k_{tri} = \frac{1}{\tau_{ri}}; \quad i = 1{,}2 \, , \tag{5}$$

and τ_1 and τ_2 are the nonradiative decay times

$$\tau_{ri} = \tau_{0i}\, exp\left(\frac{E_i}{k_B T}\right); \quad i = 1{,}2 \, , \tag{6}$$

where E_1 and E_2 are the thermal activation energies for PL quenching routes. Parameters A and B represent the ratio of the non-radiative recombination rate to radiative recombination rate.

Section S6. Fitting the temperature dependence of photoluminescence in flowing nitrogen

To confirm the fitting results in Figure 5a in the main text, we choose the PL data sets from *h*-BN covered WS_2 flakes in nitrogen and repeated the fitting by Equation S4. We have shown WS_2 is relatively stable in nitrogen gas. The activation energies obtained are $E_1 = 58.4$ meV and $E_2 = 209$ meV. The values we obtained here are close to those for PL in ambient air in the main text ($E_1 = 51.2$ meV, $E_2 = 229$ meV). In both cases, the lower activation energy E_1 represents the activation energy of exciton diffusion to the vicinity of local non-radiative recombination center. The larger excitation energy E_2 is the energy needed to unbind an exciton (to create a free exciton). It is in reasonable agreement with the binding energy of free excitons in monolayer WS_2, of 320 meV.

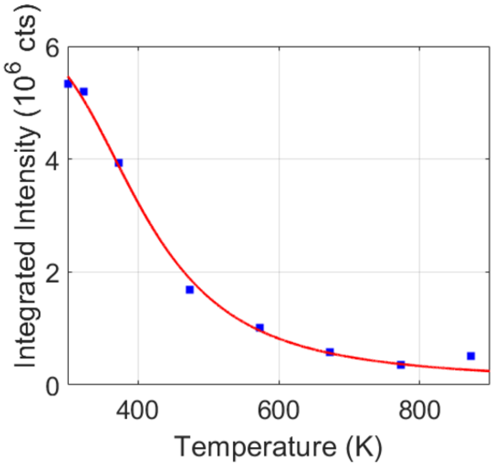

Figure S6. (a) Integrated PL intensity of the *h*-BN covered WS_2 flakes versus temperature with flowing nitrogen. The red solid red line is a curve fit to the experimental data. The experimental data are similar to those from the covered spot heating cycle in air in Figure 2a.

References

(1) Bandyopadhyay, S.; Dey, A., Convenient Detection of the Thiol Functional Group Using H/D Isotope Sensitive Raman Spectroscopy. *Analyst* **2014**, *139*, 2118-2121.

(2) Nguyen, T. P.; Lefrant, S., Raman Spectra of Silicon Monoxide. Solid State Commun. **1986**, *57*, 235-236.

(3) Nesheva, D.; Raptis, C.; Perakis, A.; Bineva, I.; Aneva, Z.; Levi, Z.; Alexandrova, S.; Hofmeister, H., Raman Scattering and Photoluminescence from Si Nanoparticles in Annealed SiO_x Thin Films. *J. Appl. Phys.* **2002**, *92*, 4678-4683.

(4) Leroux, M.; Grandjean, N.; Beaumont, B.; Nataf, G.; Semond, F.; Massies, J.; Gibart, P., Temperature Quenching of Photoluminescence Intensities in Undoped and Doped GaN. *J. Appl. Phys.* **1999**, *86*, 3721-3728.

(5) Lambkin, J. D.; Considine, L.; Walsh, S.; O'Connor, G. M.; McDonagh, C. J.; Glynn, T. J., Temperature Dependence of the Photoluminescence Intensity of Ordered and Disordered $In_{0.48}Ga_{0.52}P$. *Appl. Phys. Lett.* **1994**, *65*, 73-75.